SUPPORTING INFORMATION

A Tumor Homing Reactive Oxygen Species Nanoparticle for Enhanced Cancer Therapy

Hyeon-Yeol Cho,[†,‡,⊥] Ahmet Mavi,[§,⊥] Sy-Tsong Dean Chueng,[†] Thanapat Pongkulapa,[†] Nicholas Pasquale,[†] Hudifah Rabie,[†] Jiyou Han,[‖] Jong Hoon Kim,[¶] Tae-Hyung Kim,[,⁑] Jeong-Woo Choi,[*,‡] and Ki-Bum Lee[*,†,#]*

[†] Department of Chemistry and Chemical Biology, Rutgers, The State University of New Jersey, Piscataway, New Jersey 08854, USA

[‡] Department of Chemical & Biomolecular Engineering, Sogang University, Seoul 04107, Korea

[§] Department of Nanobiotechnology, Atatürk University, Erzurum 25030, Turkey

[‖] Department of Biological Sciences, Laboratory of Stem Cell Research and Biotechnology, Hyupsung University, Hwasung-si 18330, Korea

[¶] Department of Biotechnology, Laboratory of Stem Cells and Tissue Regeneration, College of Life Sciences and Biotechnology, Korea University, Seoul 02841, Korea

[⁑] School of Integrative Engineering, Chung-Ang University, Seoul 06974, Korea

[#] College of Pharmacy, Kyung-Hee University, Seoul 02447, Korea

[⊥] Authors made equal contributions.

* To whom correspondence should be addressed.

Prof. Tae-Hyung Kim
School of Integrative Engineering, Chung-Ang University
84 Heukseok-Ro, Dongjak-Gu, Seoul 06974, South Korea
Tel. +82-2-820-5469; Fax: +82-2-820-5940.
E-mail: thkim0512@cau.ac.kr

Prof. Jeong-Woo Choi
Department of Chemical & Biomolecular Engineering, Sogang University
35 Baekbeom-ro, Mapo-gu, Seoul 04107, South Korea
Tel. +82-2-705-8480; Fax: +82-2-3273-0331.
E-mail: jwchoi@sogang.ac.kr

Prof. Ki-Bum Lee
Department of Chemistry and Chemical Biology, Rutgers, The State University of New Jersey
610 Taylor Road, Piscataway, NJ 08854, USA
Tel. +1-732-445-2081; Fax: +1-732-445-5312
E-mail: kblee@chem.rutgers.edu

TABLE OF CONTENTS

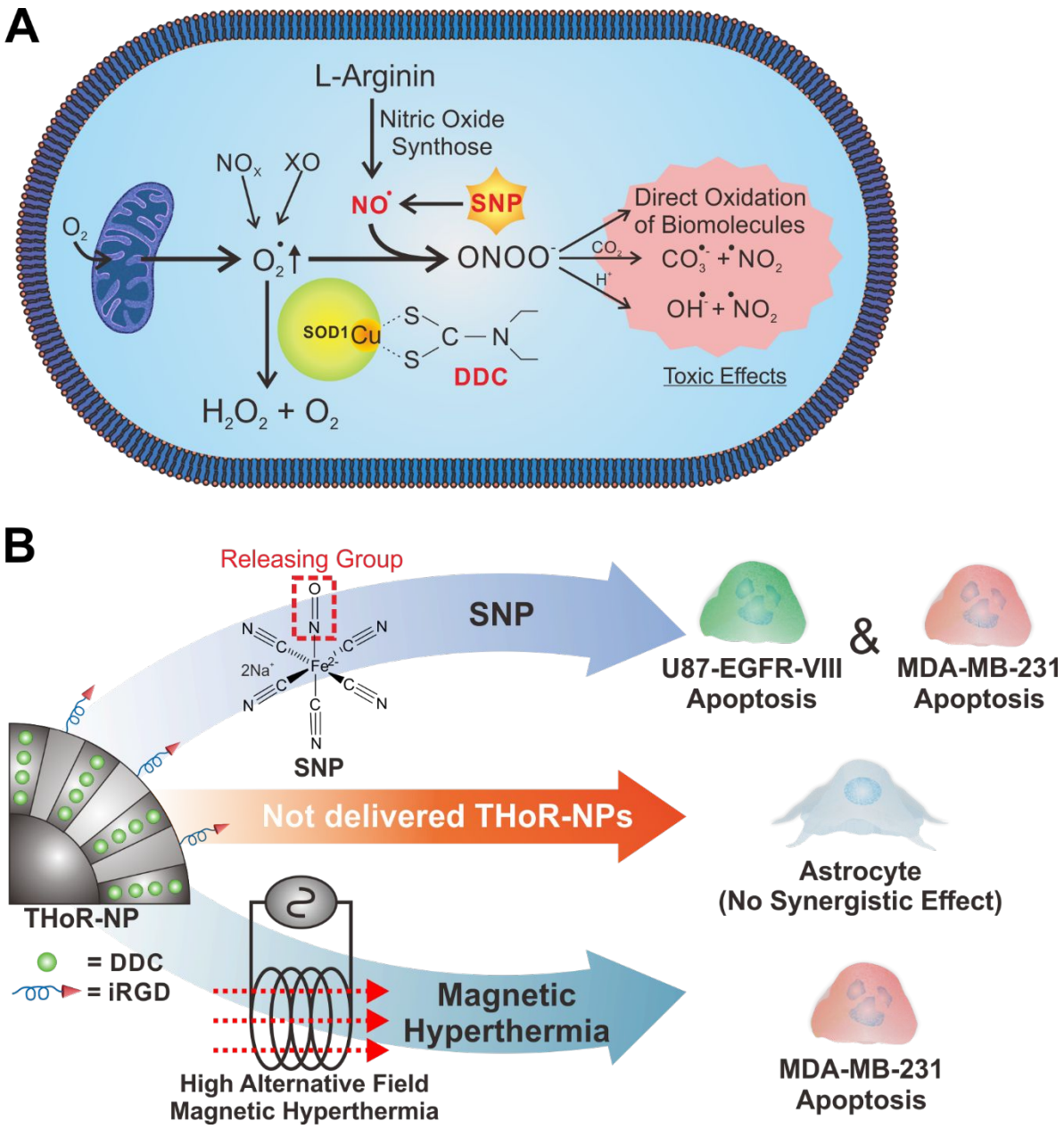

FIGURE S1: The mechanism of THOR-NP-based synergetic reactive species (ROS) generation and applications. **(A)** Intracellular mechanism of synergetic ROS based cancer therapy using both exogenous ROS-generating agents (sodium nitro preside, SNP) and ROS-scavenger inhibitor (diethyldithiocarbamate, DDC). SNP breaks down and release NO• which can generate $ONOO^-$ reacted with $O_2^{\bullet-}$. Generation of $O_2^{\bullet-}$ was accelerated with the treatment of DDC based on inhibition of superoxide dismutase 1 (SOD1). **(B)** THOR-NP composited with a magnetic core, mesoporous silica shell, and iRGD peptide can deliver the DDC into target cancer cell specifically, and it can be utilized to induce the synergetic ROS generation and to generate the magnetic hyperthermia for cancer therapy.

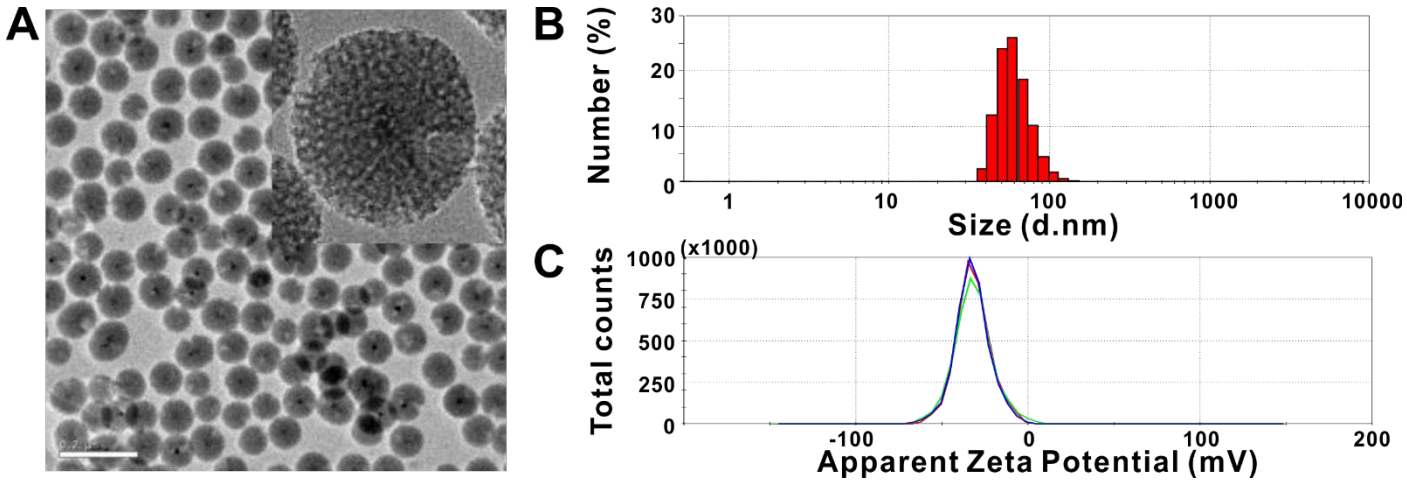

FIGURE S2: Characterization of magnetic mesoporous silica nanoparticles (MSNs). **(A)** High-resolution transmission electron microscopy (HR-TEM) revealed the monocrystalline structure of the cores and mesoporous structure of silica shell with 2-4 nm pores (scale bar: 200 nm). **(B)** The size of MSNs was monodispersed as 60 nm which determined using dynamic light scattering (DLS). **(C)** The zeta potential of non-modified MSNs was measured for further functionalization. The charge of MSN was -29 mV.

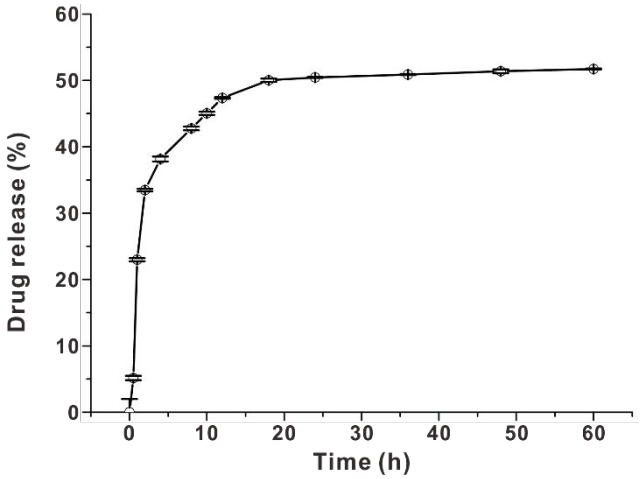

FIGURE S3: *In vitro* DDC release kinetics of DDC-loaded THoR-NPs in PBS (pH 7.4). The data represent the means ± SD of three different experiments.

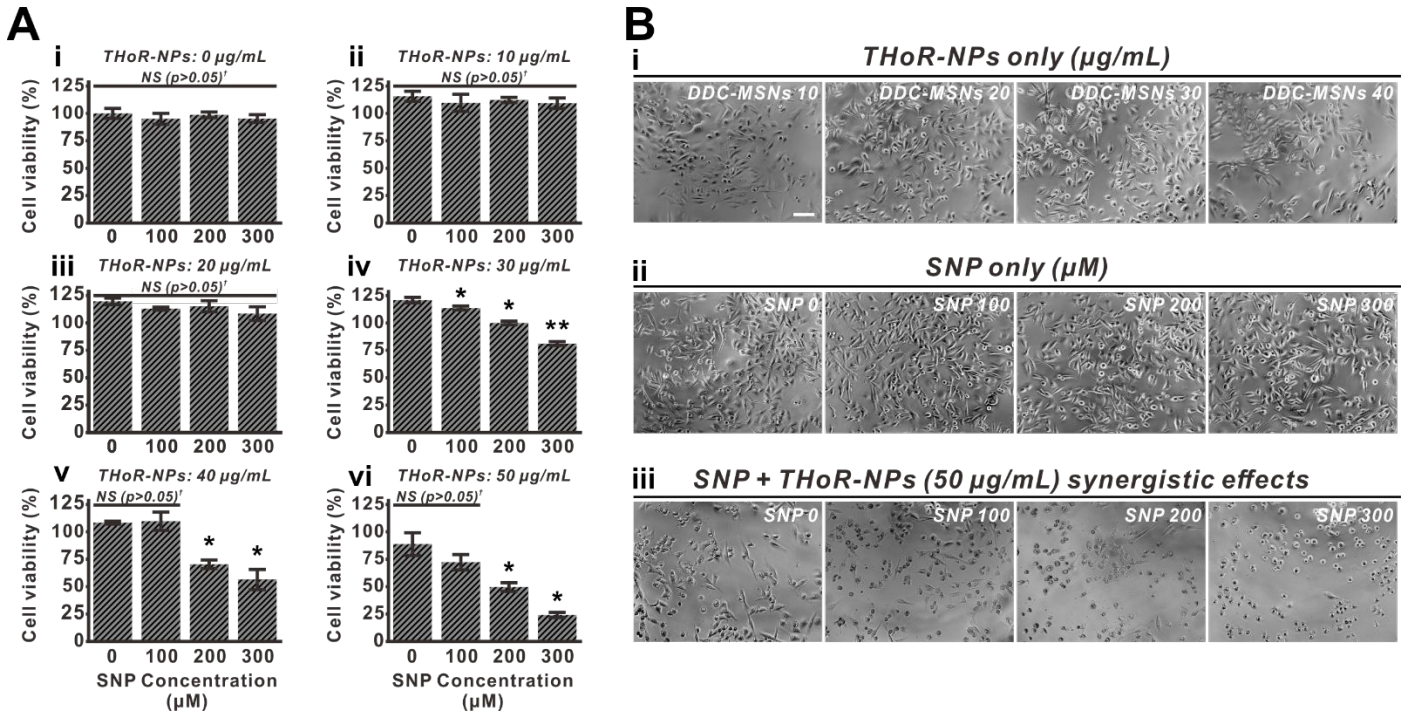

FIGURE S4: Synergistic effects of SNP and DDC on malignant breast cancer. **(A)** Dose-dependent synergistic anti-cancer effects with THoR-NP and SNP on MDA-MB-231 (malignant breast cancer cell line) determined through MTS assay. THoR-NPs is treated as 0, 10, 20, 30, 40 μg/mL and SNP is treated as 0, 100, 200, 300 μM. The data represent means ± SD of five different experiments (*$p < 0.05$, **$p < 0.01$). (B) Phage image of MDA-MB-231 cells with the combinational treatment of THoR-NPs and SNP. Scale bar: 100 μm.

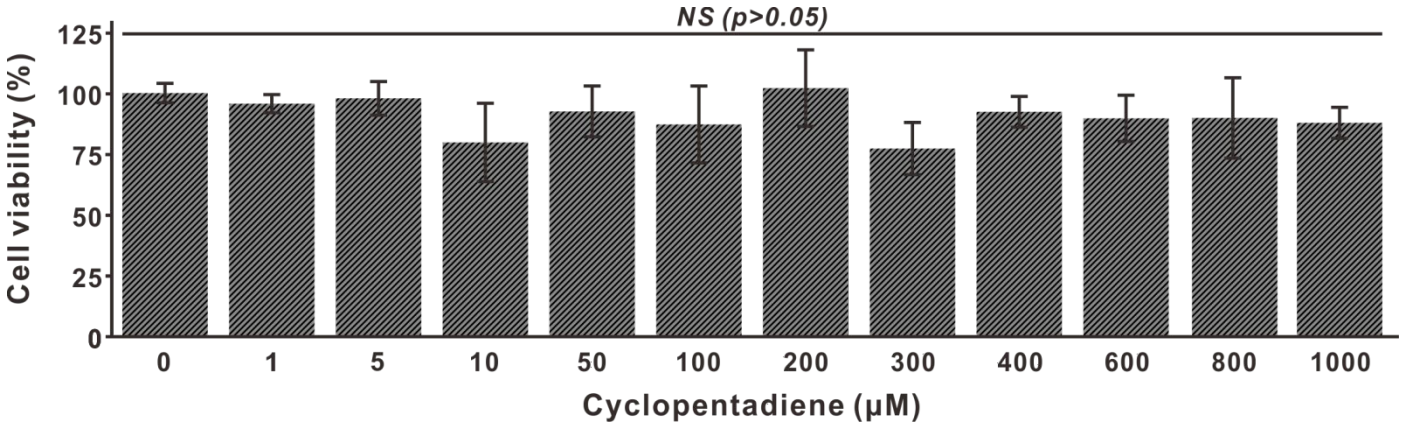

FIGURE S5: The effects of cyclopentadiene on the cancer cell. The cell viability was not affected by the increase of cyclopentadiene up to 1000 μM. The data represent means ± SD of five different experiments.

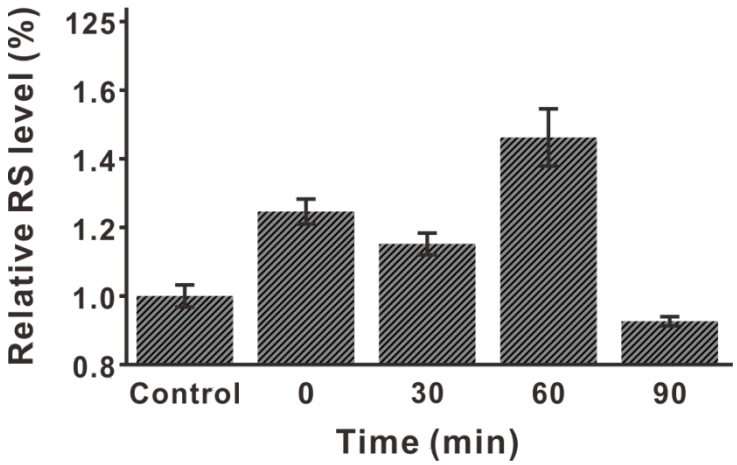

FIGURE S6: Time-dependent ROS generation of DDC-loaded MSN with magnetic hyperthermia. In the presence of the alternating magnetic field, the nanoparticles would be physically rotating and realigning themselves with the field. If bound to the cell membrane or internalized within lysosomes, these physical motions would induce stress within the cell. The ROS generation in response to these physical stresses corresponded positively with the number of nanoparticles internalized.

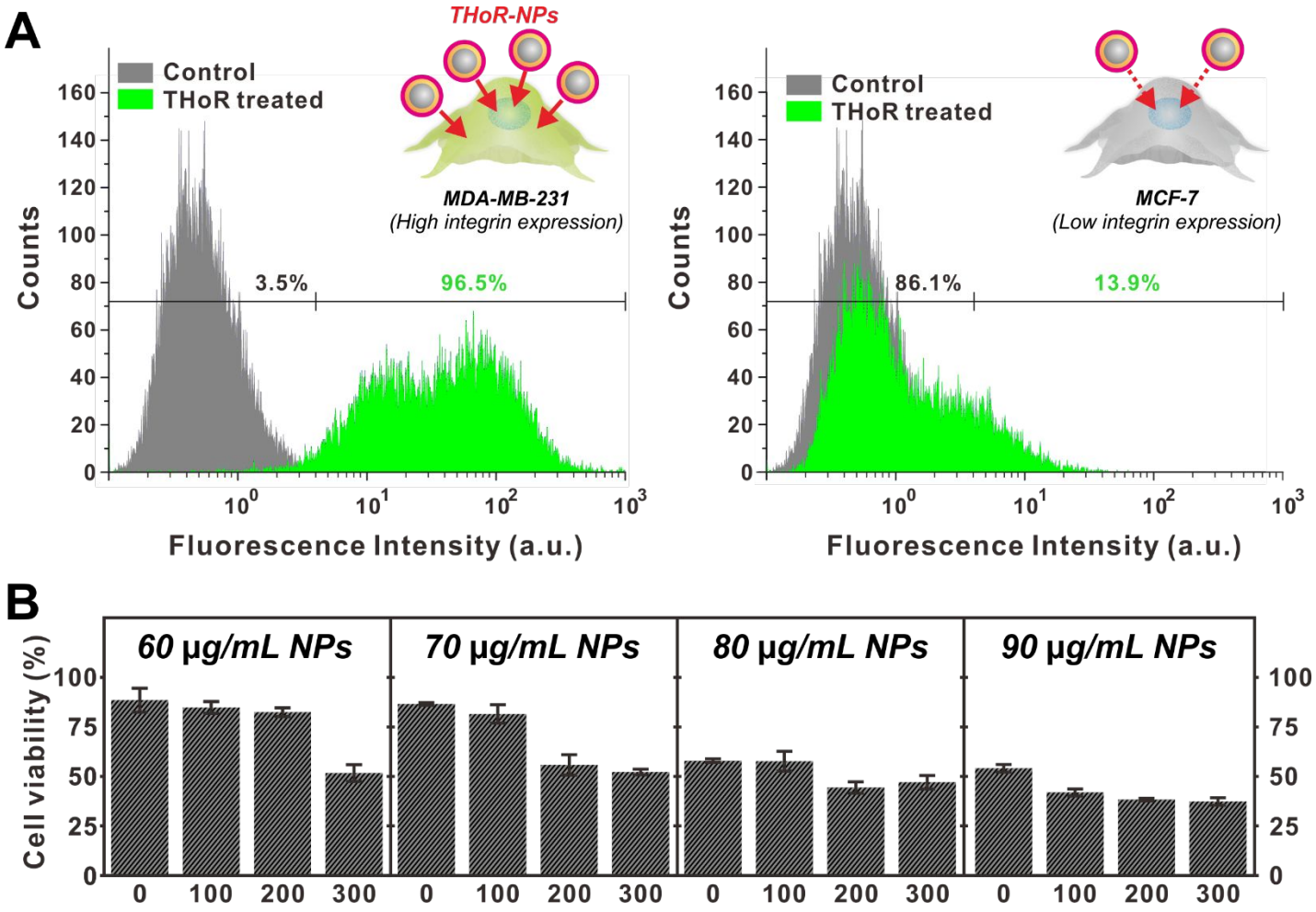

FIGURE S7: *In vitro* target-specific delivery of iRGD functionalized THoR-NPs. **(A)** Schematic diagram and flow cytometry results of integrin expression-dependent THoR-NPs cellular uptake; high (MDA-MB-231, left) and low (MCF-7, right) level of integrin expression. **(B)** Dose-dependent synergistic anti-cancer effects with THoR-NPs and SNP on MCF-7 was determined with MTS assay. THoR-NPs was treated as 60, 70, 80, and 90 μg/mL and SNP was treated as 0, 100, 200, and 300 μM.

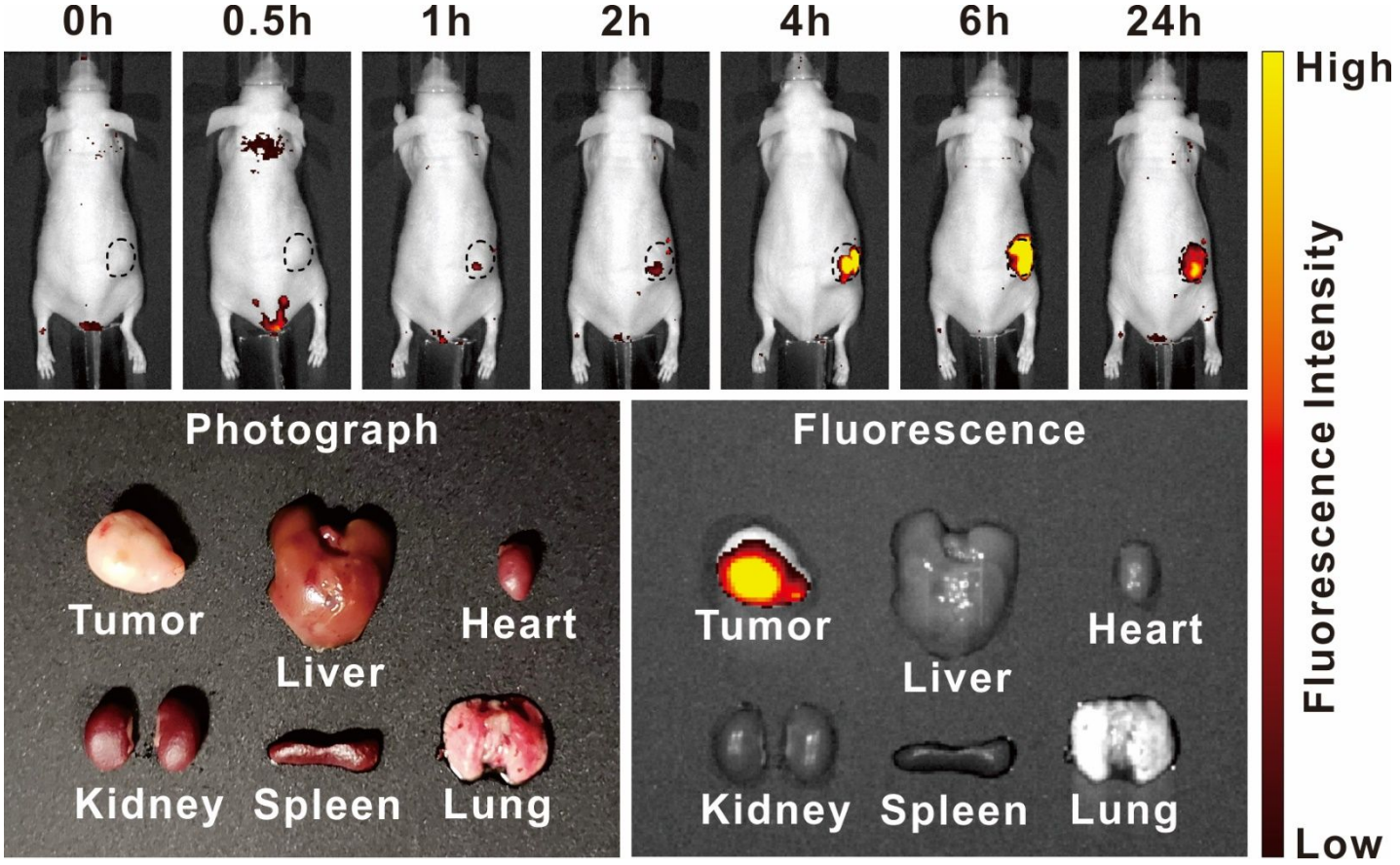

FIGURE S8: *In vivo* target-specific delivery of iRGD functionalized THoR-NPs. *In vivo* imaging (upper row) showed time-dependent THoR-NP accumulation on the tumor location for 24 hours (Black dash circle: tumor location). *Ex vivo* imaging (bottom row) supported the iRGD-based tumor-specific delivery by showing the fluorescence (FITC) signal of THoR-NPs only from the tumor.

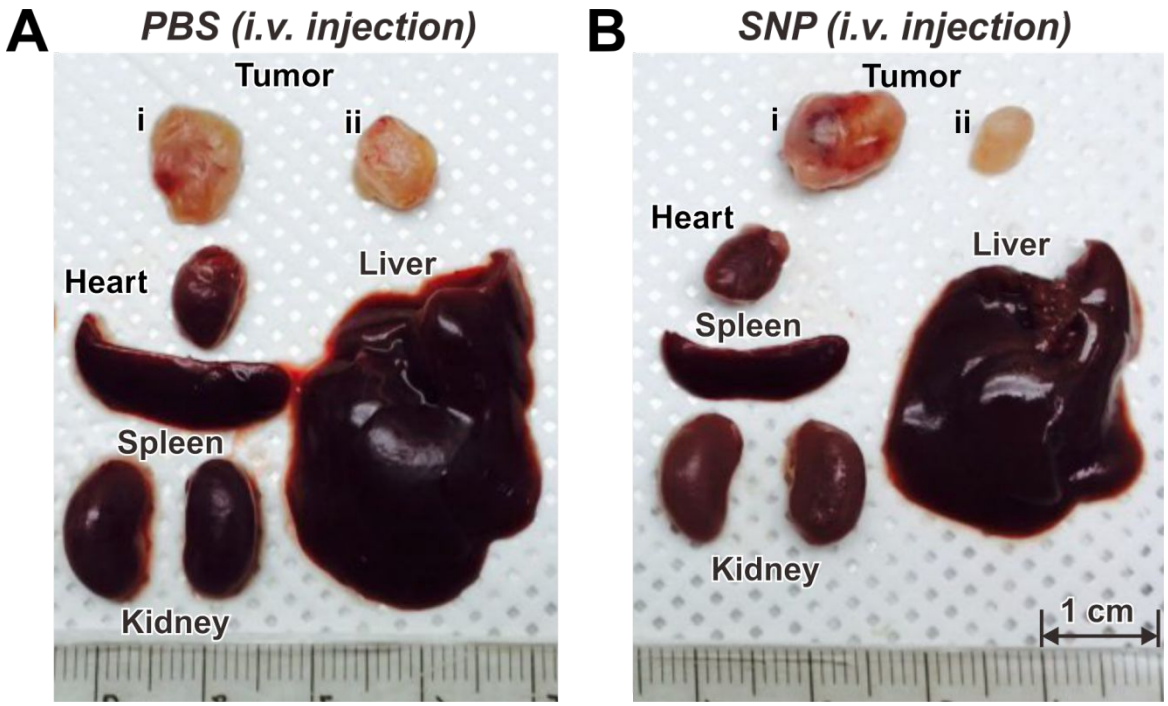

FIGURE S9: *Ex vivo* analysis of THoR-NPs and SNP combined therapy. THoR-NPs were injected intratumorally, and SNP was injected intravenously (i.v.) into a mouse weekly for four weeks; **(A)** THoR-NPs with PBS as control, **(B)** THoR-NPs with SNP. Except for the tumors, every other organ showed no damage from SNP treatment. The SNP treated mouse showed significant tumor size decrease between PBS (control, B-i) and THoR-NPs (B-ii) treatment condition while PBS-treated mouse as the control group of SNP showed similar tumor size in THoR-NP treated and non-treated conditions.

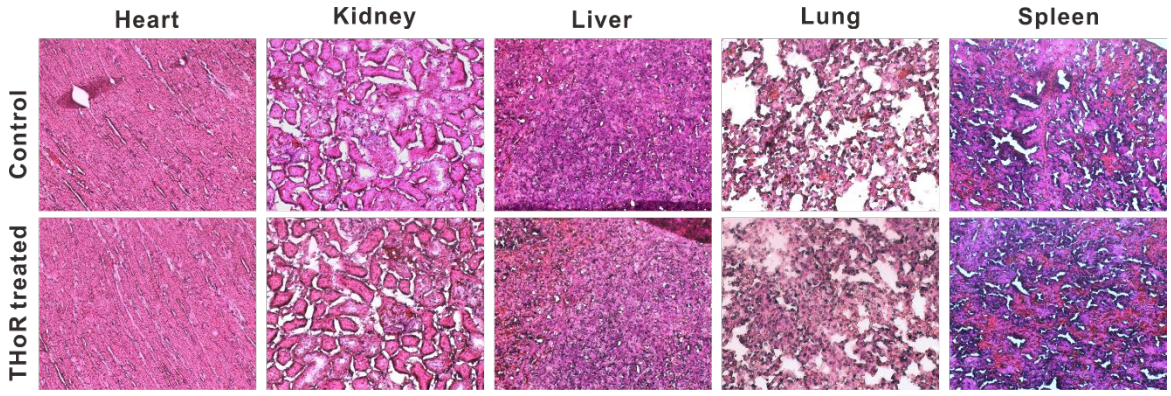

FIGURE S10: Representative H&E staining sections in various organs excised from tumor-bearing mice (Magnification: 40×).

i.v. injected SNP condition (mg/kg)	Survival rate (1 week)	Survival period
0.01	100 %	No death
0.1	100 %	No death
1	100 %	No death
10	100 %	No death
25	0 %	3 days
50	0 %	2 hours

TABLE S1: Survival period and rate of SNP injected mouse. SNP solutions were treated via intravenous (i.v.) injection with 24 h interval for 1 week and different doses; 0.01, 0.1, 1, 10, 25 and 50 mg/kg/min of SNP in 150 μL PBS. Each condition tested with 3 mice.

Targets	Forward Primer (5’-3’)	Reverse Primer (5’-3’)
GAPDH	CCGCATCTTCTTTTGCGTCG	GCCCAATACGACCAAATCCGT
CASP3	AGAGGGGATCGTTGTAGAAGTC	ACAGTCCAGTTCTGTACCACG
CASP9	CTCAGACCAGAGATTCGCAAAC	GCATTTCCCCTCAAACTCTCAA
TIMP2	GCTGCGAGTGCAAGATCAC	TGGTGCCCGTTGATGTTCTTC

TABLE S2: Table of the primers used for quantitative PCR. All primers were obtained from the PrimerBank database.